- Technical Paper -

EXPERIMENTAL STUDY ON A THREE-DIMENSIONAL RC FRAME WITH SLAB SUBJECTED TO LATERAL LOADS

Xuan DENG[*1], Toshikazu KABEYASAWA[*2], Toshimi KABEYASAWA[*3] and Hiroshi FUKUYAMA[*2]

ABSTRACT

This paper presents experimental responses of two-fifth scale three-dimensional reinforced concrete frame with floor slabs under lateral loads. The specimen was constructed with four columns and two frameworks in both directions to simulate boundary conditions of slab in real building. The damage pattern and lateral resistances of the frames in various inter-story drift angles are investigated considering the contribution of slab. It was found from the test that the slab reinforcements' participation on the beam strength was almost extended to the whole slab width even in small inter-story drift angles.

Keywords: slab participation, effective slab width, boundary condition, RC frame

1. INTRODUCTION

Current capacity design practice of high-rise building is based on the formation of a desirable beam yielding side-sway collapse mechanism realized by the inelastic behavior of structural components. However, beam flexural yielding is severely affected by slab participation, particularly when the slab is on the tension face of the beam. In practice, effective slab width is conventionally regulated in building standards and codes based on many related experimental results before. Several significant one column subassemblage tests (Suzuki, Otani and Kobayashi 1984 [1]; Joglekar 1984 [2]; Zerbe and Durrani 1985 [3]; Boroojerdi and French 1987 [4]) and frame subassemblage tests (Kokusho et al. 1988 [5]; Qi and Pantazopoulou [6]) were conducted in the 1980s and the early of 1990s.

The previous tests indicate that boundary condition has gross influence on the slab participation. Therefore, in this experiment, the specimen was constructed with four columns and two frameworks in both directions, simulating the real boundary condition of slab in real buildings. Moreover, for middle and high stories of high-rise buildings, the axial forces in the beams could be released since the columns can not restrain the elongation of the beams. A frame test was carried out under static cyclic lateral loads to investigate the hysteretic behavior with the contribution of slab. In the test, pin roller supports are installed at the base of two columns, releasing the beam axial forces. The test results have been reported elsewhere[7], while the contribution of slab to the beam resistance was discussed here in details.

2. TEST PROGRAMS

2.1 Specimen

This specimen represents the interior part of high-rise buildings' middle stories as shown in Fig. 1. Four columns of the subassemblage were extended to certain height to situate test conditions of the laboratory where this test was conducted. The beams in each direction include one span and two half-spans with floor slabs. Two end beams were added for the installation of pin supports at the ends.

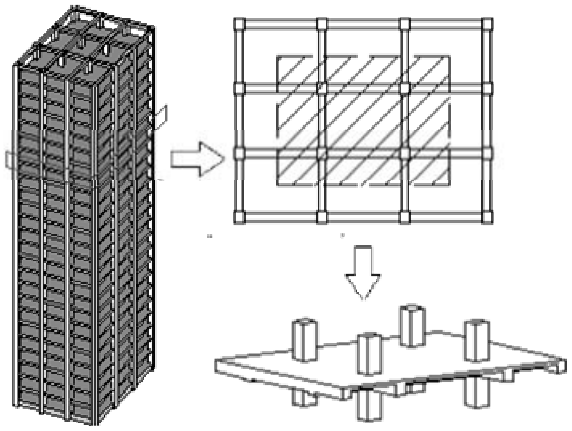

Fig. 1 Modelling concept of the specimen

The height of the specimen is 2010mm with 1085mm upper columns and 925mm lower columns measured from the beam's center axis as shown in Fig. 2. In the longitudinal direction, the center-to-center middle span is 3200mm, center-to-end half-span is 1710mm. In transverse direction, the center-to-center middle span is 2500mm, center-to-end half-span is 1100mm. The column sectional dimensions were 400mm by 400mm. The sections of the longitudinal and transverse beams were 300mm by 360mm. The sections of the transverse beam at the ends were 220mm by 290mm. The slab thickness was 100mm.

*1 Graduate School of Engineering, The University of Tokyo, JCI Member
*2 Dept. of Structural Engineering, Building Research Institute, JCI Member
*3 Earthquake Research Institute, The University of Tokyo, JCI Member

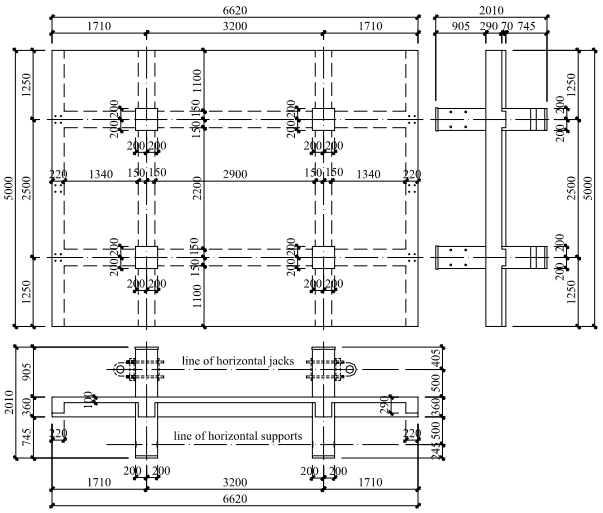

Fig. 2 Geometry of the specimen

Slab reinforcements were D6(SD295)@150 in both directions. The columns had 12-D16(SD490) as main reinforcements (the gross ratio was 1.51%) and D6(SHD685)@50 as hoops as shown in Fig. 3. The beams had 6-D16(SD490, 2 lines) as top main reinforcements and 6-D16(SD490, 2 lines) at the bottom(the gross ratio is 2.23%). The stirrups in the beams were D6(SHD685)@50. The main reinforcements of all the column and beam were anchored by welding with 40mm thick steel plates at the ends. Casting of concrete was divided into three times as in the parts of: 1)lower columns and joints, 2) beams and slabs, and 3) upper columns. The construction joints were placed about 75mm away from the column faces with wire mesh.

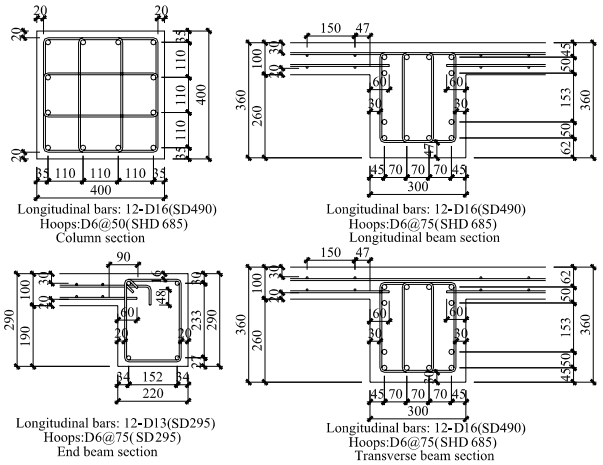

Fig. 3 Column and beam sections

2.2 Materials

In order to simulate middle stories of high-rise buildings, high strength materials were utilized in this specimen. The results of material tests are shown in the Table 1 and Table 2. Concrete's properties are illustrated by three different places respectively. The D16 bars used as the longitudinal reinforcements of beams and columns had a distinct yield plateau region, while the D6 bars used as the reinforcements of slabs and hoops did not have a yield plateau region.

Table 1 Results of concrete material tests

Concrete	Compressive strength	Strain at peak strength	Elastic Modulus	Tensional strength
	N/mm^2	μ	N/mm^2	N/mm^2
Lower columns and joints	75.98	2758	35739	5.02
Beams and slabs	65.73	2653	33072	4.85
Upper columns	67.40	2701	35083	4.61

Table 2 Results of reinforcement material tests

Steel bars	Yield strength	Yield strain	Elastic Modulus	Peak strength
	N/mm^2	μ	N/mm^2	N/mm^2
D16(SD490)	550.25	3277	204990	707.86
D6(SD295)	371.49	3981	185907	541.36
D6(SHD685)	712.82	5840	186305	910.09

2.3 Loading method

The loading setup and column labels are illustrated in Fig. 4. In order to release the beam's axial forces caused by their elongation, the column 1 and 3 were put on the pin supports, while the column 2 and 4 were put on pin roller supports. The ends of half-spans in both sides were supported by pin load cells simulating the inflection points at mid-span. In addition, two 200mm by 200mm steel beams were appended on the end beams strengthening their stiffness. Vertical jacks pined with columns could move freely by the roller supports on the top. Seismic loads were applied to all column tops by four jacks and to the pin roller supports at the bases by two jacks. The rest two base horizontal forces of column 1 and 3 could be derived by the difference of the top four jack forces and two base jack forces of column 2 and 4. Positive and negative load directions were defined in this experiment as Fig. 4.

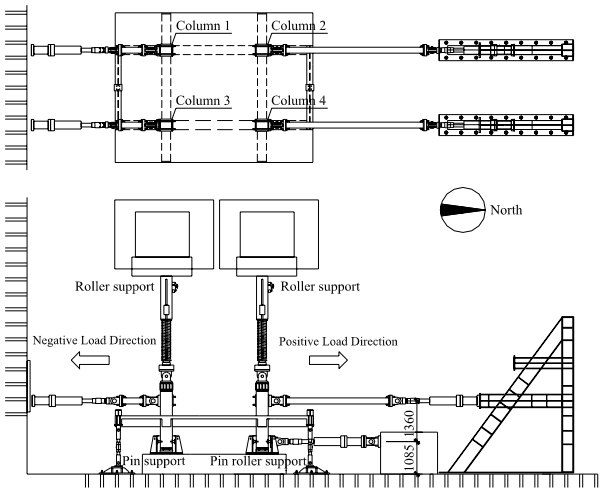

Fig. 4 Loading setup

The details of the column pin support and pin roller support at the column bases were shown in Fig. 5. Steel footing of pin support was fixed on the foundation,

while steel footing of pin roller support was just put on a smooth Teflon plate so that transversal movement was allowed. Steel rods of Φ75 welded on the steel footing were attached with the column faces to apply horizontal force or reactions. Two smooth steel curve face plates with a radius of 750mm were manufactured. One was connected to the column bottom, and another one was just put under it and could move freely with the rotation of column. Under both of them, a flat smooth steel cushion was welded on the footing. Nevertheless, in the process of test, these supports did not work well as anticipated possibly due to the friction or precision of manufacture, details of which will be discussed later in this paper.

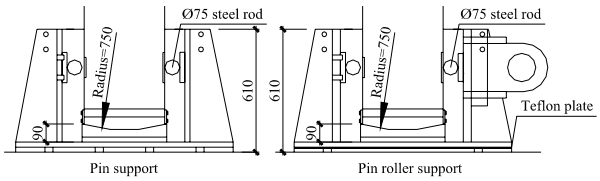

Fig. 5 Pin support and pin roller support

To simulate the vertical loads of high-rise buildings, the columns were subjected to constant axial force of 900kN each by four vertical actuators. Averaged compressive stress of the column section was 0.084 times the concrete strength. Static lateral cyclic forces were applied with six lateral oil jacks. The south jacks and north jacks were operated respectively. The story drifts were synchronized between south columns and north columns controlled manually through timely feedback data from displacement meters. Moreover, the lateral force of north horizontal top actuators and base actuators were kept almost in the same value to avoid inducing axial force in the beams. Fig. 6 shows the story drift angle history up to maximum value of 0.06rad.

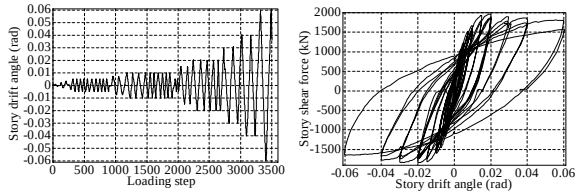

Fig. 6 Loading history and over all F-D relation

2.4 Measurement

A representative displacement meter setup (east face of west framework) is shown in Fig. 7. The story drift angle was measured by LT11 and BSL1 for column 1, LT21 and BSL2 for column 2. The beam's elongation could be obtained from LT12, LT13, LT22 and LT23 which were fixed on the steel stands beside the specimen. Column's deformation was measured in four segments by the displacement meters labelled by RC to confirm the distribution of external forces. Beam's deformation was measured in eight segments as shown in Fig. 8 (displacement meters labelled by BM). On the slab's top face, four lines of displacement meters labelled by LSL were set to measure slab deformation. Since slab reinforcement participation was investigated in this test, slab top reinforcement's strains were measured by plastic steel gauges mainly in the six sections near column 1 as displayed in Fig. 8. Meanwhile, steel strain gauges were also placed on the critical sections of beams and columns.

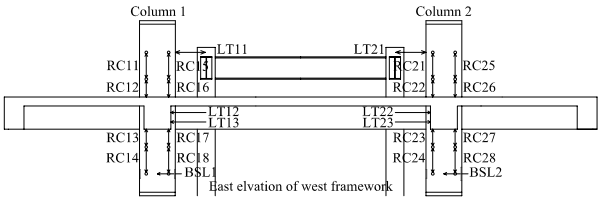

Fig. 7 Displacement meter setup of west frame

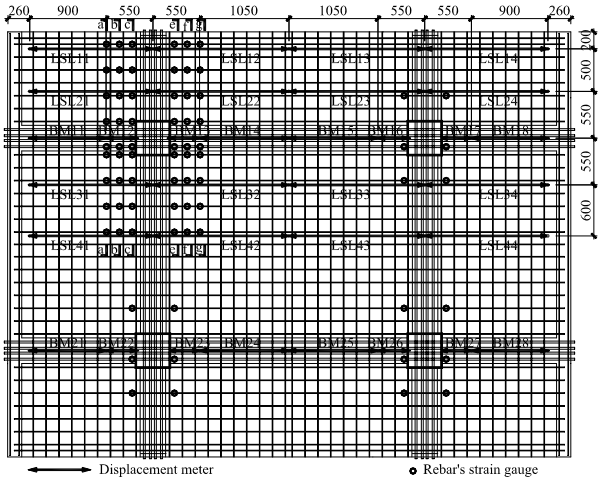

Fig. 8 The measurement of slab

3. TEST RESULTS AND DISCUSSION

3.1 Observed response

The over all hysteretic relation of story shear force and story drift angle is displayed in Fig. 6. The peak story shear force is 1963kN reached in 0.02 drift angle. After the peak point, the specimen still exhibited ductile behavior without sharp reduction in strength.

During the loading process of first loading cycle (1/1000), cracks initiated in a vertical type(bending type) from beam's bottom near joints when the story shear force are 227kN (positive load direction) and 247kN (negative load direction). All the initial cracks were about 75mm away from the column's face due to the construction joints. At the peak of 3/1000 cycles, inclined cracks (shear type) developing from beam's bottom were observed in the middle span. However, there were almost no obvious inclined cracks from the beam bottom on side half-spans in the whole loading process. This is because that the inflection point of middle span was moved to hogging moment side for slab participation, causing smaller shear span ratio that tend to generate shear cracks. The crack pattern of beam side in 1/200 cycle and 1/100 cycle were shown in Fig. 9.

In 1/100 cycle, column's cracks were founded mainly on the south and the north faces above joints, and they became more and wider with the increasing of story drift. However, no cracks were found on the column side faces below the joints in the whole process of

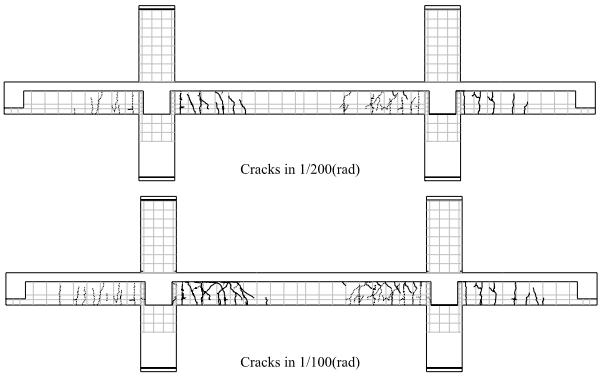

Fig. 9 Cracks on beam

the test. Moreover, it was observed that the inclination of the upper columns was larger than the lower columns, which was more obvious in larger story drift. Actually, bending moments had occurred at the base of all the columns. It also could be proved by the deformation of columns and strain of reinforcements as introduced in the next part. The formation mechanism of the moments is illustrated in Fig. 10. In the case that curve face steel plate did not move to the exact place just for a small friction force, the reaction of column's base would not locate on the center axis of column. Thus, the eccentric of bottom reaction would generate a large moment because of the high axial force in column.

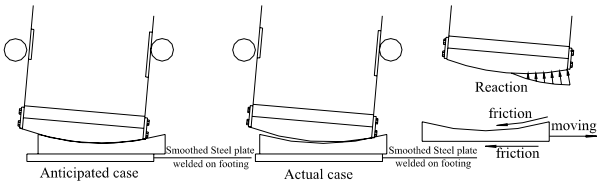

Fig. 10 Formation mechanism of base moment

The side half-spans of the transverse beams were observed having cracks on beam side near joints from 1/1000 cycle. However, these cracks were also exactly at the place of construction joints. In addition the width and number of cracks on transverse beam almost remain unchanged until 1/50 cycle. It proves that stiff boundary conditions were provided for the slab. After 1/50 cycle, inclined cracks were started to form on transverse beams and the width became wider.

The cracks in the slab were firstly observed on the top face of slab in the peak of 2/1000 cycle. However, as the initial crack in slab, it penetrated the whole width of slab immediately. Cracks on the bottom face of slab were also observed in 3.3/1000 drift of positive load direction and 2/1000 drift in the negative load direction. The cracks of middle span were perpendicular to the longitudinal beams, while cracks on the side half-spans inclined due to the different boundary conditions. The crack pattern on the slab's top face in 1/200 cycle and 1/100 cyle were displayed in Fig. 11. Another phenomenon is that when slab cracks propagated to beams, the primary cracks in vertical type would be changed to an inclined type from slab bottom.

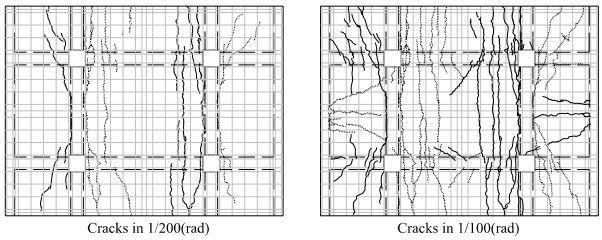

Fig. 11 Cracks on the slab's top face

3.2 Deformation and strain

Due to the column base moments, inflection points were found in the lower columns. Opposite deformation tendency was indicated between the two segments of the lower columns in Fig. 12. Strains in the main bars of the section below joints were also much less than the section above joints. Fig. 13 shows a typical strain history of the main bars in the column 1 above and below the joint.

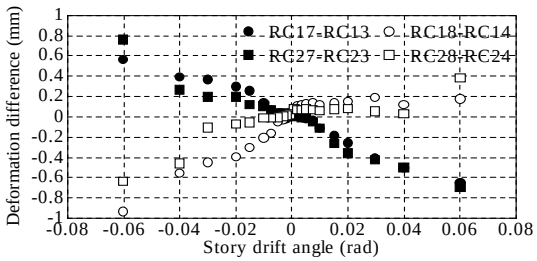

Fig. 12 Deformation difference in lower column

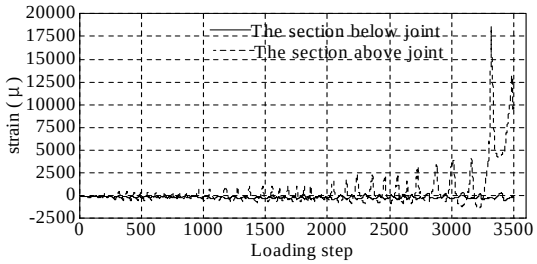

Fig. 13 Strain of column bar below and above joint

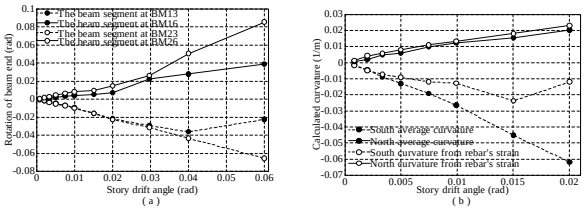

Fig. 14 Beam end rotation and curvature

The beam end rotation of middle span in positive load direction was shown in Fig. 14(a). The rotation of the hogging moment was slightly larger than sagging moment until 0.02 drift angle. According to measured strains, the beam bottom bars yielded at 0.015 drift angle, beam top bars yielded at 0.02 drift angle. Fig. 14(b) shows two types of the beam end curvatures: one was the average rotation of the 350mm length of beam end in positive load direction and another one was calculated from beam reinforcement strain at the beam end section in the positive load direction. South curvature calculated by reinforcement strain is less than averaged

obviously, which means that actual strains in the beam bottom bars were much larger than those measured by strain gauges.

Strains of the top rebars in the slab were measured at 40mm, 190mm and 340mm away from the north face of the column 1, corresponding to section e-e, f-f and g-g respectively as shown in Fig. 8. The average strain of the three sections when they are at the tension side of the slab in negative load direction was illustrated in Fig. 15. Strain of section e-e is much larger than the other two sections. The transverse strain distribution of e-e is displayed in Fig. 16. Slab strains did not decrease with the distance to the transverse direction. The sudden increase and sudden decrease were possibly induced by the large local strain at cracks.

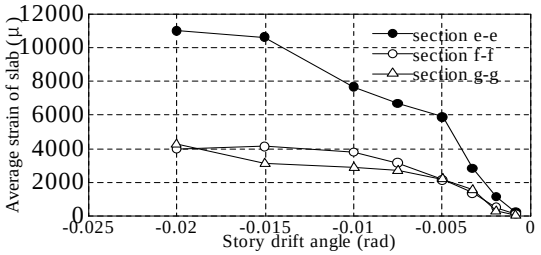

Fig. 15 Average strain of slab

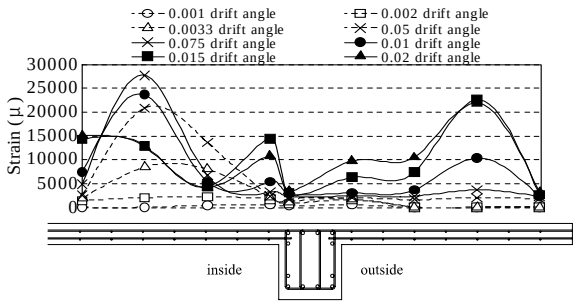

Fig. 16 Transverse distribution of slab strain

3.3 Strength of specimen

To investigate the strength of specimen, proper evaluation of the column's base moments is essential. The strains measured in the lower column bars were no more than 600μ both in tension and compression until 0.02 drift angle. Therefore, elastic curvature distribution could be assumed to the lower columns, which was proportional to the moment distribution. The force of the lower columns could be simplified as a cantilever subjected by a horizontal force F, a moment M and a axial force N as shown in Fig. 17. The rotation angles of the two segments measured by displacement meters could be used to solve the relationships between the horizontal forces and the base moments.

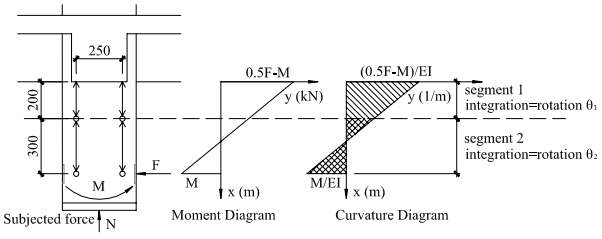

Fig. 17 Curvature distribution of lower column

Equation (1) presents the moment along the axis x in Fig. 17 and Equation (2) presents the curvature along the axis x. By integrating the curvature for the segment 1 and segment 2, the rotations of two segments θ_1 and θ_2 could be solved as Eqs. (3) and (4).

$$M(x)=F(0.5-x)-M \quad (1)$$

$$\Phi(x)=(0.5F-M-Fx)/EI \quad (2)$$

$$\theta_1=\int_0^{0.2}\Phi(x)dx=(0.08F-0.2M)/EI \quad (3)$$

$$\theta_2=\int_{0.2}^{0.5}\Phi(x)dx=(0.045F-0.3M)/EI \quad (4)$$

Here, θ_1 and θ_2 also could be derived from the deformation of column by displacement meters. Since the exact value of EI was difficult to estimate but the base horizontal forces were known, the relations of the base moment and the base horizontal force could be derived as Equation (5) through computing the ratio of θ_1 between θ_2 so that the base moment could be solved.

$$(0.08F-0.2M)/(0.045F-0.3M)=\theta_1/\theta_2 \quad (5)$$

The base moments of the column 1 and 2 were calculated from Eq. (5) at the first peaks of the loading cycles as shown in Fig. 18. The moments at the lower section under the joint in the column 1 were derived from these calculated base moments as shown in Fig. 20. To confirm the reliability of these calculated results, another method, computing the moment by the strains of column main bars were also implemented. Linear strain distribution was assumed at the section as Fig. 19. Since the strains of rebars were small, the moment of the section was mainly induced by the stress of concrete. Here, concrete was supposed elastic and without tensional force. The maximum compressive strain of bars was used to estimate the strain of concrete because in compression slip of rebar tended to let rebar strain smaller than concrete strain. Then, other strain distributions were estimated from the strain at this point and the total axial force. Based on this method, the whole column section was in compression until 0.0075 story drift angle like case A in Fig. 19. After that, the stress distribution of the section was like case B. The section moments derived by measured strains were obtained as also shown in Fig. 20. The figure indicates that both estimation methods gave close results. After the determination of the column base moments, the whole mom-

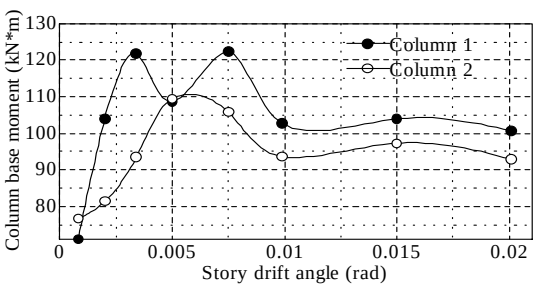

Fig. 18 Column base moment

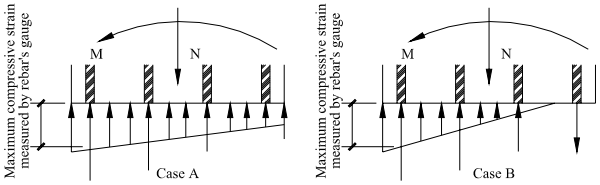

Fig. 19 Assumed stress distribution of column

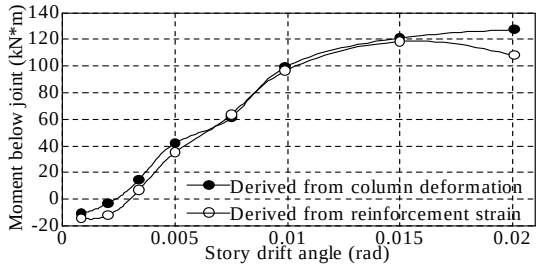

Fig. 20 Moment of the section below joint

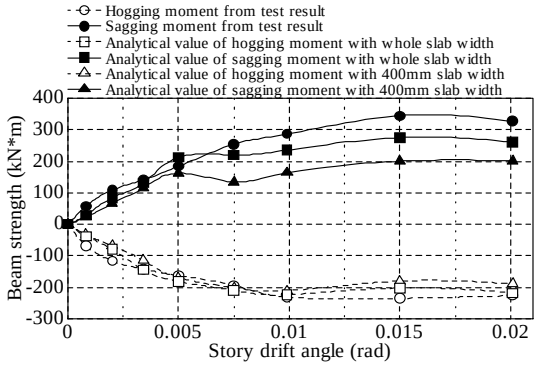

Fig. 21 Beam strength-story drift angle relationship

ent distribution could be obtained including the beam ends. Fig. 21 shows the south end moment (hogging moment) and the north end moment (sagging moment) in positive load direction.

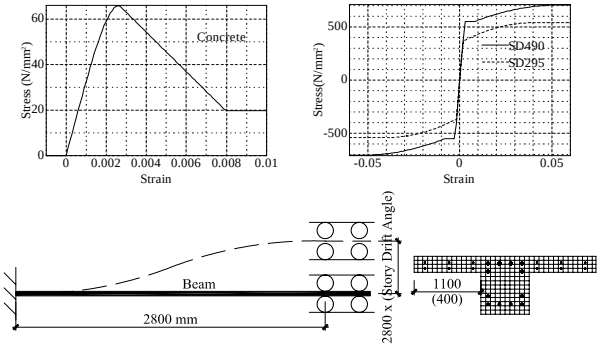

Fig. 22 Analytical model

In order to evaluate the beam strength of the test results, flexural analysis was carried out with beam model shown in Fig. 22 and fiber model at the section. Dual-roller support was defined on the right side to let the beam elongate freely. The constitutive laws of concrete and reinforcements utilized in this analysis are also shown in Fig. 22. Two cases were taken into consideration for the comparison with the test results, one was a T shape beam with whole slab width, another was the T shape beam with 400mm slab each side (In Japanese code, 1m slab effective width was always considered in the secondary design, here the scale 2/5 was multiplied). Peak strength of the test was higher than the analysis probably because of large local reinforcement hardening at cracks, which could not be reflected by the usual fiber model.

4. CONCLUSIONS

(1) Crack pattern of slab in a frame subjected by lateral load was obviously influenced by boundary condition. For interior part of buildings, the sagging moments tend to produce straight cracks perpendicular to transverse beam on slab.

(2) The transverse strains measured in the slab along the beam critical section did not decrease with the increase of transverse distance from the beam.

(3) From the beam strengths estimated from the test and the flexural analysis, the equivalent effective slab width was almost the whole width even in small story drift angle.

ACKNOWLEDGEMENT

This test was conducted in the Large Size Experiment Laboratory of Building Research Institute, and was supported by many related people in ERI, BRI and Ohbayashi-Gumi LTD.

REFERENCES

[1] Suzuki, N., Otani, S. and Kobayashi, Y., “Three-Dimensional Beam-Column Subassemblages under Bidirectional Earthquake Loadings,” Proceedings, Eighth World Conference on Earthquake Engineering, V. 6, San Francisco, Prentice-Hall, Inc., 1984, pp.453-460

[2] Joglekar, M. et al., “Full Scale Tests of Beam-Column Joints,” Publication SP - American Concrete Institute, 1985, pp.271-304

[3] Zerbe, H. E., and Durrani, A. J., “Effect of Slab on the Behavior of Exterior Beam to Column Connections,” Report No. 30, Department of Civil Engineering, Rice University, Houston, Tex., 1985

[4] French, C. W., and Boroojerdi, A., “Contribution of R.C. Floor Slabs in Resisting Lateral Loads,” Journal of Structural Engineering, ASCE, Vol. 115, No. 1, 1989, pp.1-18

[5] Sakata, H. and Wada, A., “Experiments on Reinforced Concrete One-twentieth Scale Model Frames : A Study on Elastic and Plastic Behaviors of Reinforced Concrete Frames In Consideration Of Axial Elongation in Bending Yield Beams,” Journal of Structural and Construction Engineering, Transactions of AIJ (403), Sep. 30, 1989, pp.45-55

[6] Qi, X. and Pantazopoulou, S.J., “Response of Rc Frame under Lateral Loads,” Journal of Structural Engineering, ASCE, Vol. 117, No. 4, April 1991, pp.1167-1188

[7] Toshikazu Kabeyasawa, Hiroshi Fukuyama, Hideo Katshumata, Kuniyoshi Sugimoto, Toshimi Kabeyasawa, Deng Xuan: Static loading test of a three-dimensional frame simulating highrise reinforced concrete building structures (No.1: Outline of the test), Proceedings, AIJ Annual Convention, 2011, pp.741-742.